Continuous-wave, multimilliwatt, mid-infrared source tunable across 6.4–7.5 μm based on orientation-patterned GaAs

Kavita Devi,[1,*] P. G. Schunemann,[2] and M. Ebrahim-Zadeh[1,3]

[1]*ICFO—Institut de Ciencies Fotoniques, Mediterranean Technology Park, 08860 Castelldefels, Barcelona, Spain*

[2]*BAE Systems, Inc., MER15-1813, P.O. Box 868, Nashua, New Hampshire 03061-0868, USA*

[3]*Institucio Catalana de Recerca i Estudis Avancats (ICREA), Passeig Lluis Companys 23, Barcelona 08010, Spain*

**Corresponding author: kavita.devi@icfo.es*

Received October 1, 2014; accepted October 26, 2014;
posted October 31, 2014 (Doc. ID 224218); published December 1, 2014

We report a continuous-wave (cw) source of tunable mid-infrared radiation providing tens of milliwatt of output power in the 6460–7517 nm spectral range. The source is based on difference-frequency generation (DFG) in orientation-patterned (OP)-GaAs pumped by a Tm-fiber laser at 2010 nm and a 1064 nm-Yb-fiber-pumped cw optical parametric oscillator. Using a 25.7-mm-long OP-GaAs crystal, we have generated up to 51.1 mW of output power at 6790 nm, with >40 mW and >20 mW across 32% and 80% of the mid-infrared tuning range, respectively, which is to the best of our knowledge the highest tunable cw power generated in OP-GaAs in this spectral range. The DFG output at maximum power exhibits passive power stability better than 2.3% rms over more than 1 h and a frequency stability of 1.8 GHz over more than 1 min, in high spatial beam quality. The system and crystal performance at high pump powers have been studied.

OCIS codes: (140.3070) Infrared and far-infrared lasers; (190.2620) Harmonic generation and mixing; (190.4360) Nonlinear optics, devices; (190.4400) Nonlinear optics, materials; (190.4970) Parametric oscillators and amplifiers; (140.3510) Lasers, fiber.

http://dx.doi.org/10.1364/OL.39.006751

Continuous-wave (cw) laser light sources with extended tunability in the mid-infrared (mid-IR) are of considerable interest for a diverse range of applications, including spectroscopy and trace gas detection [1,2]. In particular, the 6–8 μm wavelength range is attractive for medical and biological applications [3]. With the scarcity of solid-state lasers, quantum cascade lasers (QCLs) are viable sources, capable of providing hundreds of mW of cw power in the mid-IR [4]. However, wide tuning together with narrow linewidth still remain limitations. As such, for practical generation of widely tunable cw radiation in the mid-IR, nonlinear optical techniques based on difference-frequency generation (DFG) [2] and optical parametric oscillators (OPOs) [5] still represent a highly effective approach. The cw OPOs based on MgO-doped periodically poled $LiNbO_3$ (MgO:PPLN) are now firmly established as the most effective approach for the generation of tunable high-power radiation up to ~4 μm [6], with wavelengths up to 5 μm also obtained at the mW power level [7]. However, the intrinsic onset of absorption in MgO:PPLN and other oxide-based ferroelectric materials beyond ~4 μm presents a fundamental barrier to wavelength generation at practical powers further into the mid-IR. As such, the search for alternative nonlinear materials with high transmission above ~4 μm and effective techniques for spectral expansion into the longer mid-IR wavelengths must be explored.

In this context, orientation-patterned (OP)-GaAs is a highly attractive nonlinear crystal. Its high nonlinear coefficient ($d_{\text{eff}} = d_{14} \sim 94$ pm/V) [8], wide transparency across 0.9–17 μm, high thermal conductivity (46 W/mK), and high damage threshold [9] make it a primary candidate for deep mid-IR generation. Its nonlinear figure of merit, $F = d_{\text{eff}}^2/n^3$ (n is the refractive index), is nearly ten times that of MgO:PPLN. In an early report, a pulsed OPO based on OP-GaAs, tunable in the 5.7–9.1 μm range was demonstrated, using a PPLN OPO pumped by a Q-switched Nd:YAG laser at 1064 nm [10]. Recently, a pulsed OP-GaAs OPO tunable over 8.8–11.5 μm was reported using direct pumping with a Q-switched Tm, Ho:YLF laser [11]. However, the development of cw OPOs at wavelengths >4 μm still remains a major challenge, in a large part due to the high threshold sensitivity to cavity loss in practical singly resonant configuration, combined with the difficulty in achieving relatively complex mirror and crystal coatings of high quality and low loss in the deep mid-IR spectral range to achieve oscillation threshold. In the meantime, one can circumvent this obstacle by deploying the alternative technique of DFG, which is single-pass and does not require the attainment of an oscillation threshold. The technique can provide an effective and robust approach for the generation of non-negligible output powers at longer wavelengths [2]. In the past few years, DFG based on OP-GaAs, with cw output powers up to several μW has been demonstrated [12]. A few years ago, a cw source tunable across 7.6–8.2 μm with sub-mW output power was reported by using DFG between an Er-doped fiber source and a Tm-doped fiber laser in OP-GaAs [13]. Although these sources provide coverage across an important spectral range of interest in the deep mid-IR, the attainment of high output power, leading to noise-free, pure spectral output is yet to be demonstrated. In this Letter, we report the generation of multitens of mW level output power in the spectral range of 6.4–7.5 μm by exploiting DFG between a high-power Yb-fiber-pumped cw OPO and a cw Tm-fiber laser in OP-GaAs. Today, cw OPOs based on MgO:PPLN are well established as practical and reliable sources of tunable radiation in the mid-IR capable of delivering watt-level output power across 2–4 μm [6,14]. With further

advances in fiber laser technology, high-power cw Tm-fiber lasers at ~2 μm are also now becoming commercially available with improving performance for nonlinear frequency conversion applications [15]. Hence, the combination of tunable watt-level cw MgO:PPLN OPOs and high-power Tm-fiber lasers can be effectively exploited to achieve wavelength generation into the deep mid-IR at practical powers, and with wide tunability, using the DFG technique. By deploying such a scheme in OP-GaAs, we have generated cw radiation across 6460–7517 nm, with as much as 51.1 mW of output power at 6790 nm and >40 mW across 32% of tuning range, in TEM_{00} spatial mode profile, with good power and frequency stability. To the best of our knowledge, these are the highest cw powers generated with OP-GaAs, with broad tunability in the deep mid-IR.

The schematic of the experimental setup is shown in Fig. 1. The first pump source used is a commercial cw Tm-fiber laser (IPG Photonics, TLR-50-2010-LP), delivering up to 43 W of output power at 2010 nm in a linearly polarized beam with a quality factor of $M^2 = 1.2$. The linewidth of the laser, measured using an optical spectrum analyzer with a resolution of 0.1 nm, is ~1.5 nm. The second pump source is a home-built cw OPO based on an earlier design [6], but using a 38-mm-long MgO:PPLN, pumped by a commercial cw Yb-fiber laser (IPG Photonics, YLR-30-1064-LP-SF) at 1064 nm. The OPO is singly resonant for the signal, and provides tunable output across 2.4–2.9 μm in the nonresonant idler, with as much as 4.9 W of cw power at $\lambda_i = 2748$ nm for grating period of $\Lambda_{MgO:PPLN} = 31.5$ μm. The OPO signal linewidth at $\lambda_s = 1683.9$ nm, measured using an optical spectrum analyzer, is $\Delta\lambda_s = 0.9$ nm, limited by the instrument resolution. However, given the single-frequency nature of the cw Yb-fiber pump laser ($\Delta\lambda \sim 89$ kHz), the generated signal and idler are expected to also be single-frequency. The Tm-fiber laser is operated at maximum power, and the input power, P_1, for DFG is adjusted using a combination of a half-wave plate (H_1) and a polarizing beam splitter (PBS). A second half-wave plate (H_2) is used to control the pump polarization for phase-matching in the DFG crystal. The output power from the OPO, P_2, is adjusted by varying the Yb-fiber pump power using a combination of a half-wave plate and a polarizing beam-splitter cube [6]. For DFG, we used 25.7-mm-long, 9-mm-wide, 2.1-mm-thick OP-GaAs crystal with grating period of $\Lambda_{OP\text{-}GaAs} = 63.5$ μm. The crystal has antireflection (AR)-coated end-faces over 2000–8000 nm ($R < 18\%$) and is housed in an oven with stability of ±0.1°C, which can be controlled from room temperature to 200°C. The pump beams, P_1 and P_2, are both *e*-polarized, allowing type 0 ($ee \rightarrow e$) phase-matching for DFG in the OP-GaAs crystal. The lenses, $L_{1,2}$ and $L_{3,4}$, are used to adjust the beam diameters, while mirrors $M_{2,3}$ and $M_{4,5}$ are used to optimize spatial overlap of the two beams, P_1 and P_2, on lens, L_5, respectively. Mirror, M_5, is reflective ($R > 90\%$) for P_2, while highly transmitting ($T > 99\%$) for P_1. The lens, L_5, of focal length, $f = 300$ mm, is used to focus P_1 and P_2 to waist radii of $w_1 \sim 49$ μm and $w_2 \sim 62$ μm, corresponding to confocal focussing parameters of $\xi_1 = 1.02$ and $\xi_2 = 0.92$, respectively, at the center of the OP-GaAs crystal ($b_1 \sim b_2$). Dichroic mirror, M_6, is used to separate P_1, while filter F_1 is used to separate P_2, from the generated DFG beam. To reject any residual P_1 and P_2 while recording the DFG power, we used an additional filter, F_2.

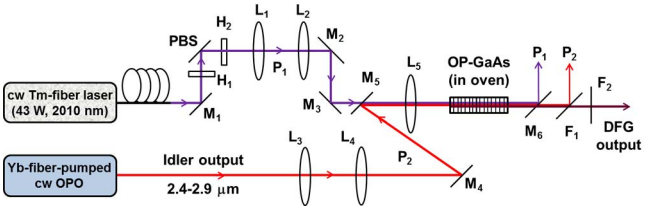

Fig. 1. Schematic of the experimental setup. PBS, polarizing beam splitter; $H_{1,2}$, half-wave plates; L_{1-4}, lenses; M_{1-6}, mirrors; $F_{1,2}$, filters.

The DFG spectral tuning in the mid-IR in the present device is achieved by tuning the OPO idler wavelength. To study the DFG tuning range, we varied the temperature of the MgO:PPLN crystal, T_{OPO}, and simultaneously adjusted the phase-matching temperature, T_{DFG}, of the OP-GaAs crystal, at maximum pump powers. By varying T_{OPO} from 40°C to 105°C, and T_{DFG} from 38.5°C to 190.5°C, we were able to achieve DFG tuning across 6460–7517 nm. Figure 2(a) shows the measured DFG wavelengths using a wavemeter (Bristol 721 Spectrum Analyzer) with absolute accuracy of ±1 ppm for mid-IR, and the calculated values using energy conservation ($\nu_1 - \nu_2 = \nu_{DFG}$, where ν_1, ν_2, and ν_{DFG} are the frequencies of the Tm-fiber, OPO idler, and DFG output, respectively), as a function of OPO idler wavelength. As evident from the plot, we were able to obtain continuous DFG spectral coverage over ~1050 nm by tuning the OPO idler wavelength over only ~170 nm. Figure 2(b) shows the measured DFG tuning range, together with the calculated curve using the Sellmeier equations for OP-GaAs [16], as a function of the crystal temperature. The slight discrepancy in the DFG phase-matching temperature is attributed to the heating of the OP-GaAs crystal at higher input pump powers.

We measured the generated DFG output power across the mid-IR for a fixed available Tm-fiber laser power

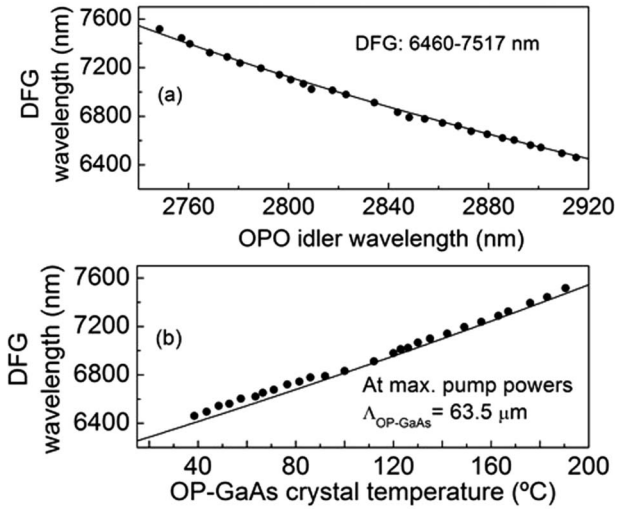

Fig. 2. Measured (filled circle) and calculated (solid line) (a) DFG tuning range across the OPO idler wavelength and (b) DFG wavelength versus the OP-GaAs crystal temperature.

of 36.7 W, and fixed maximum OPO idler power at any given idler wavelength, at the input to the OP-GaAs crystal. The results are shown in Fig. 3, where it can be seen that the generated DFG was continuously tunable across the entire 6460–7517 nm range, providing >40 mW and >20 mW over 32% and 80% of the full DFG spectral coverage, respectively, with a maximum of 51.1 mW at $\lambda_{DFG} = 6790$ nm. The data correspond to the generated power at the exit face of the OP-GaAs crystal, after correction for a total transmission loss of ~20% through the dichroic mirror, M_6, and the two filters, F_1 and F_2. The drop in the DFG power at the center of the tuning range is due to the corresponding drop in the OPO idler power, owing to the maximum absorption coefficient of the OH-vibration peak at 2826 nm in the MgO:PPLN crystal [17]. The inset of Fig. 3 shows the corresponding maximum OPO idler power available for DFG across the tuning range. The DFG power across the tuning range follows a similar behavior to the input OPO idler power, except at longer DFG wavelengths. This is attributed to the increased reflectivity of the AR coating on the OP-GaAs crystal, as well as reduced transmission of dichroic mirror, M_5, at longer DFG wavelengths.

To further investigate the performance of the mid-IR cw DFG device, we performed power scaling measurements, while maintaining one of the input pump powers fixed at the maximum. Keeping the Tm-fiber power fixed at 36.7 W, and increasing the OPO idler power by increasing the Yb-fiber pump power, we recorded the DFG output power at $\lambda_{DFG} = 6543$ nm as a function of input OPO idler power. The result is shown in Fig. 4(a). The DFG power increases linearly with the input OPO idler power, reaching as high as 47.6 mW. While performing the power scaling measurement, T_{DFG} was adjusted as the OPO idler power was varied, because of the change in the OPO idler wavelength with the increase in the Yb-fiber pump power. As shown in the inset of Fig. 4(a), T_{DFG} increases from 45°C to 48.5°C with the increase in the input OPO idler power to maximum, while the idler wavelength simultaneously decreases from 2910.5 to 2900.9 nm. We then recorded the variation of DFG output power with the increase in Tm-fiber power, while keeping the OPO idler power fixed at the maximum value of 2.9 W at $\lambda_i = 2901$ nm. The result is shown in Fig. 4(b). As evident, the DFG output power has a similar linear dependence on the Tm-fiber pump power. While increasing the laser pump power, T_{DFG} was adjusted to generate

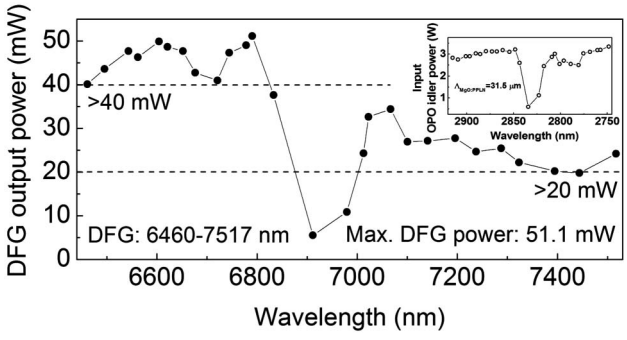

Fig. 3. Variation of DFG power across the tuning range, at maximum pump powers. Inset: corresponding input OPO idler power available for DFG across the tuning range.

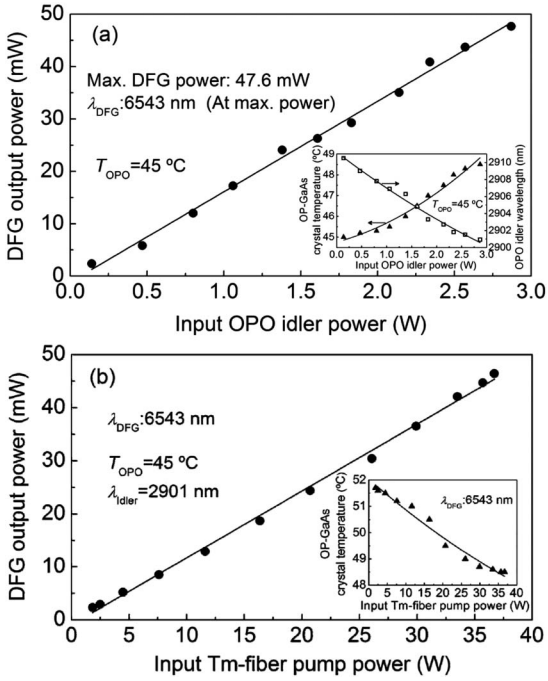

Fig. 4. Dependence of the measured cw DFG power at 6543 nm on (a) incident OPO idler power and (b) incident Tm-fiber pump power. Solid lines are guide to the eye. Insets: (a) OP-GaAs quasi-phase-matched temperature, and the corresponding OPO idler wavelength, as a function of OPO idler power. (b) OP-GaAs crystal temperature as a function of laser pump power at $\lambda_{DFG} = 6543$ nm. Solid lines are guide to the eye.

maximum DFG power at $\lambda_{DFG} = 6543$ nm. As shown in the inset of Fig. 4(b), T_{DFG} decreases from 51.7°C to 48.5°C, with the increase in the Tm-fiber pump power, due to the heating of the OP-GaAs crystal at high pump powers. We also investigated stronger and looser focusing for both beams, P_1 and P_2, with smaller beam waist radii ($w_1 \sim 35$ μm, $w_2 \sim 45$ μm) and larger beam waist radii ($w_1 \sim 88$ μm, $w_2 \sim 110$ μm), respectively, at the center of the OP-GaAs crystal, by changing the focal length of lens, L_5. However, this resulted in lower DFG output power, which could be due to the reduced spatial overlap of P_1 and P_2 beams within the OP-GaAs crystal.

We then recorded the passive power stability of the DFG output at 6604 nm at the maximum input pump powers, under free-running conditions. The result is shown in Fig. 5, where the generated mid-IR power is recorded to exhibit a passive stability better than 2.3% rms over >1 h. The instability in power is attributed to the mechanical vibrations and air currents in the laboratory and possible mode-hopping in the OPO in the absence of active stabilization. The DFG power stability is expected to be improved with active control of the OPO, as well as thermal and mechanical-vibration isolation of the system. The inset of Fig. 5 shows the near-field energy distribution of the mid-IR output beam at 6604 nm, at maximum pump powers, recorded using Pyrocam III camera. The result confirms excellent spatial quality with a beam circularity >95%. Similar profiles were obtained across the entire DFG tuning range. Moreover, we have not observed any degradation in the beam quality, nor damage to the OP-GaAs crystal or the AR coating, after sustained long-term operation.

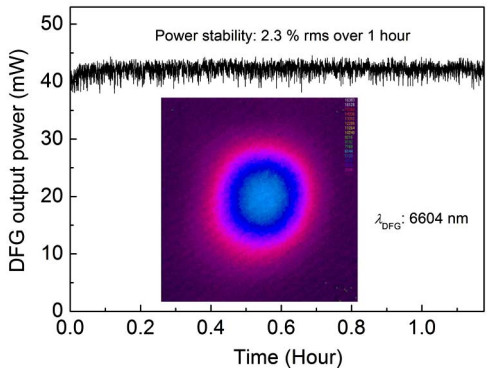

Fig. 5. DFG output power stability at maximum power over more than 1 h. Inset: near-field TEM_{00} energy distribution of the generated DFG beam.

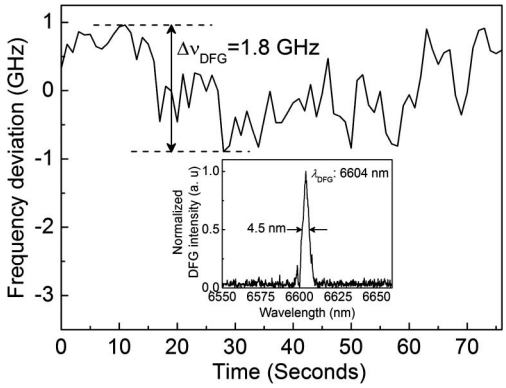

Fig. 6. Frequency stability of DFG output at maximum power over more than 60 s. Inset: DFG spectrum.

We also investigated the frequency stability of the generated cw mid-IR radiation by recording the DFG frequency as a function of time using a wavemeter (Bristol 721) at maximum power. The result is shown in Fig. 6. Under free-running conditions and in the absence of thermal isolation, the DFG output exhibits a peak-to-peak frequency deviation of $\Delta\nu_{DFG} = 1.8$ GHz over >1 min, with a central wavelength of 6590.1494 nm. With better isolation of the system, and active stabilization of OPO and Tm-fiber laser wavelength, further improvements in the frequency stability of the mid-IR output are expected. Also shown in the inset of Fig. 6 is the DFG spectrum at $\lambda_{DFG} = 6604$ nm, measured using a spectrum analyzer (Bristol 721), with a spectral resolution of 6 GHz in the mid-IR. As can be seen, the spectrum has a FWHM linewidth of 4.5 nm (~30 GHz). The measured frequency stability also indicates the narrow linewidth of the DFG output.

In conclusion, we have demonstrated a tunable source of cw radiation for the mid-IR, providing multitens of mW output power in the 6460–7517 nm spectral range, for the first time to the best of our knowledge. To achieve such high powers, together with a broad tuning range, we have exploited single-pass DFG between a high-power cw Tm-fiber laser and an Yb-fiber-pumped cw OPO in OP-GaAs. The system provides up to 51.1 mW of cw power in the deep mid-IR, in high beam quality, with good passive power and frequency stability. The output power can be further increased with higher cw OPO idler powers using a longer (~80 mm) MgO:PPLN crystal, and improved AR coatings on the OP-GaAs crystal. Given the great interest in the wavelength regions of 4–6 μm and 8–12 μm, the atmospheric transmission window for safety and security applications, by using an OP-GaAs crystal with grating periods of ~57 and ~69 μm, and OPO idler wavelengths across 3.08–3.96 μm and 2.58–2.72 μm, the obtained tuning range can be further extended to 4.0–5.7 μm and 7.7–9.0 μm, respectively, using the same cw Tm-fiber laser at 2010 nm. With thermal and mechanical isolation, and electronic control of the OPO pump source, the power and frequency stability of the DFG output can be further enhanced. These features make the device a promising source of tunable cw radiation in the deep mid-IR for a variety of applications.

We acknowledge support from the Ministry of Economy and Competitiveness (MINECO), Spain, through project OPTEX (TEC2012-37853), and the European Office of Aerospace Research and Development (EOARD) through grant FA8655-12-1-2128.

References

1. A. Elia, C. Di Franco, P. M. Lugara, and G. Scamarcio, Sensors **6**, 1411 (2006).
2. W. Chen, J. Cousin, E. Poullet, J. Burie, D. Boucher, X. Gao, M. W. Sigrist, and F. K. Tittel, C.R. Physique **8**, 1129 (2007).
3. C. E. Webb and J. D. C. Jones, *Handbook of Laser Technology and Applications: Applications* (CRC Press, 2004).
4. F. Capasso, Opt. Eng. **49**, 111102 (2010).
5. M. Ebrahim-Zadeh and I. T. Sorokina, eds., *Mid-Infrared Coherent Sources and Applications* (Springer, 2008), pp. 347–375.
6. S. Chaitanya Kumar, R. Das, G. K. Samanta, and M. Ebrahim-Zadeh, Appl. Phys. B **102**, 31 (2011).
7. M. M. J. W. van Herpen, S. E. Bisson, and F. J. M. Harren, Opt. Lett. **28**, 2497 (2003).
8. T. Skauli, K. L. Vodopyanov, T. J. Pinguet, A. Schober, O. Levi, L. A. Eyres, M. M. Fejer, J. S. Harris, B. Gerard, L. Becouarn, E. Lallier, and G. Arisholm, Opt. Lett. **27**, 628 (2002).
9. A. Grisard, E. Lallier, and B. Gérard, Opt. Mater. Express **2**, 1020 (2012).
10. K. L. Vodopyanov, O. Levi, P. S. Kuo, T. J. Pinguet, J. S. Harris, M. M. Fejer, B. Gerard, L. Becouarn, and E. Lallier, Opt. Lett. **29**, 1912 (2004).
11. R. K. Feaver, R. D. Peterson, and P. E. Powers, Opt. Express **21**, 16104 (2013).
12. S. E. Bisson, T. J. Kulp, O. Levi, J. S. Harris, and M. M. Fejer, Appl. Phys. B **85**, 199 (2006).
13. S. Vasilyev, S. Schiller, A. Nevsky, A. Grisard, D. Faye, E. Lallier, Z. Zhang, A. J. Boyland, J. K. Sahu, M. Ibsen, and W. A. Clarkson, Opt. Lett. **33**, 1413 (2008).
14. K. Devi, S. Chaitanya Kumar, A. Esteban-Martin, and M. Ebrahim-Zadeh, Opt. Express **20**, 19313 (2012).
15. K. Devi, S. Chaitanya Kumar, and M. Ebrahim-Zadeh, Opt. Express **19**, 11631 (2011).
16. T. Skauli, P. S. Kuo, K. L. Vodopyanov, T. J. Pinguet, O. Levi, L. A. Eyres, J. S. Harris, M. M. Fejer, B. Gerard, L. Becouarn, and E. Lallier, J. Appl. Phys. **94**, 6447 (2003).
17. J. M. Cabrera, J. Olivares, M. Carrascosa, J. Rams, R. Müller, and E. Diéguez, Adv. Phys. **45**, 349 (1996).